

Localization-delocalization transition of a reaction-diffusion front near a semipermeable wall

Bastien Chopard

Computer Science Department, Université de Genève, CH-1211 Genève 4, Switzerland

Michel Droz and Jérôme Magnin

Département de Physique Théorique, Université de Genève, CH-1211 Genève 4, Switzerland

Zoltán Rácz

Institute for Theoretical Physics, Eötvös University, 1088 Budapest, Puskin ulica 5-7, Hungary

(Received 27 June 1997; revised manuscript received 19 August 1997)

The $A+B\rightarrow C$ reaction-diffusion process is studied in a system where the reagents are separated by a semipermeable wall. We use reaction-diffusion equations to describe the process, and to derive a scaling description for the long-time behavior of the reaction front. Furthermore, we show that a critical localization-delocalization transition takes place as a control parameter which depends on the initial densities and on the diffusion constants is varied. The transition is between a reaction front of finite width that is localized at the wall and a front which is detached and moves away from the wall. At the critical point, the reaction front remains at the wall but its width diverges with time (as $t^{1/6}$ in the mean-field approximation). Below two dimensions, the fluctuations play an important role and the critical exponents have no longer their mean-field values. [S1063-651X(97)12311-X]

PACS number(s): 82.20.Wt, 82.20.Db, 82.20.Mj, 66.30.Ny

I. INTRODUCTION

Reaction fronts formed in diffusion-limited $A+B\rightarrow C$ -type reactions have been investigated intensively in recent years [1–19]. The motivation came partly from the realization that moving reaction fronts play an important role in a great variety of physical and chemical phenomena which display pattern formation [20–23]. Another reason for the interest is the simplicity of the problem, which allows the application of different theoretical approaches. Indeed, front properties have been studied in detail by using mean-field and scaling theories [6], dynamical renormalization group calculations [14], and numerical simulations [24], and in some cases exact analytical predictions have also been made [13].

In most of the cases studied previously, the reaction front formed after the spatially separated components A and B came into contact. For example, in a typical experiment aimed at producing Liesegang bands [25], one has a vertical tube of gel soaked with component B , and, at time $t=0$, a liquid containing the reagent A is poured over the gel (in order to eliminate convection effects, the liquid is sometimes replaced with another gel containing A). The theoretical equivalent of this situation is that the reagents are separated by a wall which is removed at $t=0$, and then the reaction-diffusion process begins.

One can imagine, however, that there are situations when the wall between the reagents is present at all times, and this wall is semipermeable, allowing only one of the reagents to pass through. It may happen, for example, in the above-discussed setup, that B is not soluble in the liquid containing A , which is effectively equivalent to the presence of a semipermeable wall. More importantly, chemical reactions in biological systems usually take place in strongly inhomogeneous media with semipermeable walls present [27–29].

Thus we believe it is important (hence the aim of this paper) to consider the formation of reaction fronts in systems with initially separated species when the wall separating the two species is not eliminated at $t=0$, but is replaced by a semipermeable wall, which allows only one of the reagents (A) to diffuse across.

Using a mean-field description of the above process, we find that the control parameter in this system is given by

$$r = 1 - \frac{b_0 \sqrt{D_b}}{a_0 \sqrt{D_a}}, \quad (1)$$

where a_0 and b_0 are the initial particles densities, while D_a and D_b are the diffusion coefficients. We show that, depending on the sign of r , three distinct types of behavior occur. When $r>0$, the A particles invade the B phase. The reaction front moves away from the semipermeable wall, with the distance from the wall increasing as \sqrt{t} , and the wall is irrelevant in the long-time regime. Thus one recovers the predictions (e.g., the width of the reaction zone scales as $w\sim t^{1/6}$) made with no semipermeable wall present [1]. In the opposite case, $r<0$, the wall prevents the B particles from invading the A region and, accordingly, the reaction front becomes localized (with finite width) at the semipermeable wall. It turns out that the dividing point between the $r>0$ and $r<0$ cases is a critical point in the sense that the width of the reaction zone diverges at $r=0$. We have thus found a critical localization-delocalization transition from a reaction front localized at the wall to a front detached and moving away from the wall. It should be noted that a localization-delocalization transition of the reaction zone in a related $A+B\rightarrow C$ reaction process has already been discussed by Richardson and Evans [26]. They considered finite-size systems with an injection of hard-core A and B particles at opposing ends of a one-

dimensional lattice, and assumed bulk driving for each species in the opposite directions. Changing the injection rate or the reaction rate, they observed sharp transitions between states with localized and delocalized reaction zones. The localization-delocalization transition we discuss takes place in a purely diffusive $A+B\rightarrow C$ system and, as we shall see below, the presence of the membrane plays a crucial role in the existence of the phenomenon. Nevertheless, there is some similarity between transitions in these systems, in that they can be related to boundary effects. This is not so surprising, however, since boundary conditions are at the heart of most of the nonequilibrium transitions.

Our results described above will be derived and discussed first by defining the model (dynamical equations and the boundary conditions) in Sec. II. Then the different regimes are analyzed (Sec. III) both analytically and numerically at the mean-field level. The role of the fluctuations is discussed in Sec. IV, and concluding remarks are given in Sec. V.

II. MODEL

The basic notions about reaction zones have been introduced for the $A+B\rightarrow C$ process [1] and, in order to keep the discussion transparent, we shall also consider this case. More complicated reaction schemes $\nu_A A + \nu_B B \rightarrow C$ can be treated along the same line, with the same general picture arising.

We shall assume that the transport kinetics of the reagents is dominated by diffusion and that the reaction kinetics is of second order. Thus, at a mean-field level, the mathematical description of the process is given in terms of reaction-diffusion equations

$$\partial_t a = D_a \nabla^2 a - kab, \quad (2)$$

$$\partial_t b = D_b \nabla^2 b - kab, \quad (3)$$

where a and b are the densities of the reagents A and B , respectively, D_a and D_b are the corresponding diffusion constants, and the reaction-rate parameter is k . Note that there is a conservation law in this system. Since the A and B particles react in pairs, the difference in their numbers is conserved. In terms of the densities, this means that the spatial integral of $a-b$ is constant unless there are particle sources at the boundaries.

The semipermeable membrane is located at the $(x=0, y, z)$ plane. Initially, all B particles are on the right-hand side of this membrane ($x>0$), and, since the membrane is impenetrable for them, they remain on that side for all times. In terms of the particle density b , this means that the solution of Eqs. (2) and (3) must satisfy the conditions

$$b(x<0, t) = 0, \quad \left. \frac{\partial b(x, t)}{\partial x} \right|_{x=0^+} = 0. \quad (4)$$

The motion of the A particles is not influenced by the membrane and, initially, they are on the left side of it. Furthermore, the initial densities are assumed to be constant, i.e., $a(x, 0) = a_0$ and $b(x, 0) = 0$ for $x < 0$ while $a(x, 0) = 0$ and $b(x, 0) = b_0$ for $x > 0$. With this choice of initial state, the solution of Eqs. (2) and (3) depends only on the x spatial coordinate, and the system effectively becomes one dimensional.

Our aim will be to calculate the production rate of C particles defined by

$$R(x, t) = ka(x, t)b(x, t), \quad (5)$$

and investigate the time evolution of its spatial structure with emphasis on the center

$$x_f(t) = \int_{-\infty}^{\infty} xR(x, t)dx \Big/ \int_{-\infty}^{\infty} R(x, t)dx, \quad (6)$$

and the width of the reaction zone,

$$w(t) = \left[\int_{-\infty}^{\infty} (x-x_f)^2 R(x, t)dx \Big/ \int_{-\infty}^{\infty} R(x, t)dx \right]^{1/2}. \quad (7)$$

Both x_f and w are easily measurable quantities in experiments and simulations.

III. SCALING PROPERTIES OF THE FRONT

For a system without the membrane, it is known [3,17] that the reaction front will move to the right (A invades B) or to the left (B invades A) depending on the relative magnitude of quasistationary diffusive currents ($J^A \sim D_a a_0 / \sqrt{D_a t}$ and $J^B \sim D_b b_0 / \sqrt{D_b t}$), i.e., depending on the sign of the control parameter r :

$$r = 1 - \frac{J^B}{J^A} = 1 - \frac{b_0 \sqrt{D_b}}{a_0 \sqrt{D_a}}. \quad (8)$$

For $r = r_c = 0$, the front is stationary in the sense that, although $R(x, t)$ remains time dependent for large times, the center of the reaction zone does not move and $x_f(t \rightarrow \infty)$ approaches a finite constant.

One expects that the direction of invasion plays an important role in the presence of the membrane as well and, accordingly, we shall analyze the $r > 0$, $r < 0$, and $r = 0$ cases separately.

A. $r > 0$: Invasion of the free (A) reagents—delocalized front

For $r > 0$, the diffusive current of A particles overwhelms the corresponding current of B particles, and thus the reaction front moves to the right. After a while, the B particles disappear from the neighborhood of the membrane, and thus the membrane does not play a role anymore. Consequently, the reaction front leaves the membrane (Fig. 1) and all the results about the long-time scaling form of the reaction front obtained previously apply [1], namely,

$$R(x, t) \sim t^{-\beta} F\left(\frac{x-x_f}{t^\alpha}\right), \quad (9)$$

where the position of the center of the front, x_f , scales with time as $x_f \sim \sqrt{t}$, the width of the reaction front is proportional to t^α with $\alpha = \frac{1}{6}$, the scaling exponent of the production rate of C at $x = x_f$ is $\beta = \frac{2}{3}$, and the scaling function $F(z)$ is a fast decreasing function for $z \rightarrow \pm \infty$. We can call this front delocalized since both the center and the width of the front diverge in the long-time limit. In closing this subsection, we note that the above results are modified by fluctuations in

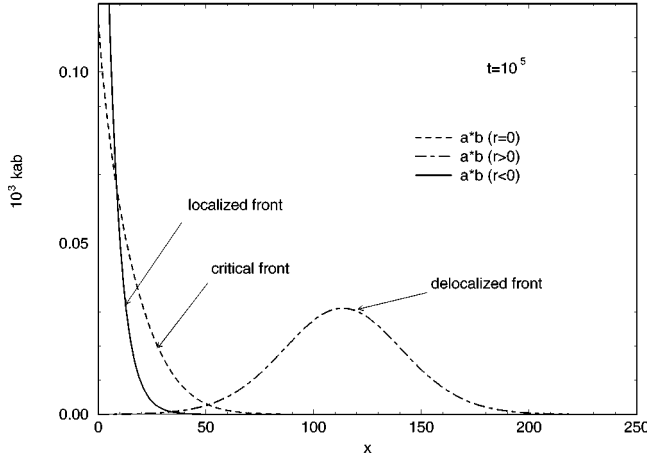


FIG. 1. Production rate of C near the semipermeable membrane (localized at $x=0$) for three different values of the control parameter r . The width of the localized front is stationary, while the width of the critical front increases with time as $t^{1/6}$. The distance between the delocalized reaction front and the membrane increases as $t^{1/2}$, while its width diverges as $t^{1/6}$. Time is measured in units of $\tau=0.1/(ka_0)$, where k is the reaction rate and a_0 is the initial density of A . The unit of length is chosen to be $l=\sqrt{D_a\tau}$, where D_a is the diffusion coefficient of A .

low dimensions ($d<2$), as discussed in several works on $A+B\rightarrow C$ reactions without the presence of a membrane [6,13].

B. $r<0$: Invasion of the blocked (B) reagents—localized front

For $r<0$, the B particles would be the invading particles, but they cannot penetrate past the membrane. Thus one expects that there will be a finite density of B particles at $x=0$ and, consequently, that A particles can penetrate into the $x>0$ region only up to a finite distance ξ . In order to make this picture (Fig. 2) quantitative, we shall first solve the prob-

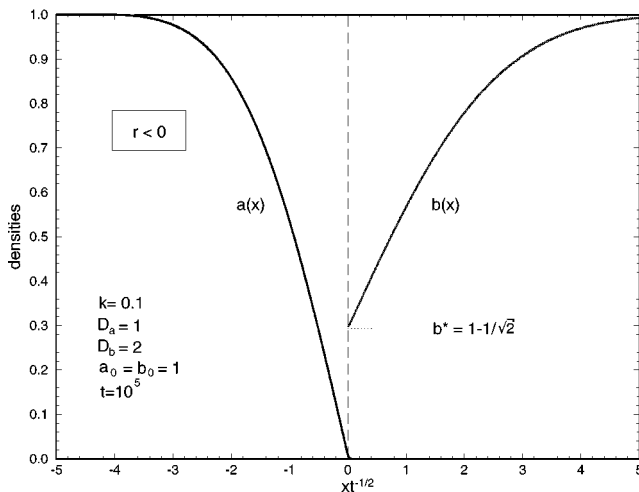


FIG. 2. Density profile of the reagents for $r<0$ as seen on a diffusive scale ($x\sim t^{1/2}$). For the given values of diffusion coefficients (D_a, D_b) and initial densities (a_0, b_0), the large time limit of b at $x=0$ is given by $b^*=1-1/\sqrt{2}$. The units are those defined in Fig. 1.

lem on the diffusive length scale $x\sim\sqrt{t}$, and then use this solution as the large-argument asymptotics of the solution around $x=0$.

Viewing the process on the diffusive length scale, the reaction zone is reduced to a point ($x=0$), and the diffusion of A and B takes place separately in the $x<0$ and $x>0$ regions. The appropriate boundary conditions are as follows:

$$a(x\rightarrow-\infty, t)=a_0, \quad a(0, t)=0, \quad (10)$$

$$b(x\rightarrow\infty, t)=b_0, \quad -D_a \left. \frac{\partial a}{\partial x} \right|_{x=0^-} = D_b \left. \frac{\partial b}{\partial x} \right|_{x=0^+}. \quad (11)$$

The first boundary conditions in Eq. (10) and (11) are obvious, while the second boundary condition in Eq. (11) is just the expression of the equality of the currents entering the reaction zone. The second condition in Eq. (10) is more complicated. It follows from the assumption that the penetration length ξ is finite combined with the fact that the diffusion current approaches zero at large times, [$J_{\text{diff}}\sim D_a(\partial a/\partial x)|_{x=0}\rightarrow 1/\sqrt{t}$, i.e., the derivative $(\partial a/\partial x)|_{x=0}$ diminishes for $t\rightarrow\infty$]. The finiteness of ξ , in turn, follows from the finiteness of $b(0, t)=b^*$, and so, finding b^* finite at the end of our calculation provides a self-consistency check of the underlying picture.

The solution of the diffusion equations with the above boundary conditions is given by

$$a(x, t)=-a_0\text{Erf}(x/\sqrt{4D_a t}), \quad (12)$$

$$b(x, t)=b^*+(b_0-b^*)\text{Erf}(x/\sqrt{4D_b t}), \quad (13)$$

where $\text{Erf}(x)$ is the error function [30], and $b^*=b(0, t)$ is found from the second condition in Eq. (11):

$$b^*=b_0-a_0\left(\frac{D_a}{D_b}\right)^{1/2}=-a_0\left(\frac{D_a}{D_b}\right)^{1/2}r. \quad (14)$$

As we can see, b^* is indeed finite for finite $r<0$ ($b^*>0$ because it has the meaning of particle density).

The above results are valid on length scale $x\sim t^{1/2}$. In order to investigate the details of the reaction zone, we must consider the $x\sim t^0$ region (Fig. 3), where we should find a solution with large-distance asymptotics which matches to the solution found above.

Since we are mainly interested in finding the extent of the region where the reaction product appears, we should find the region of penetration of A particles into the $x>0$ half-space. For $x\ll\sqrt{t}$, one can approximate $b(x, t)\approx b^*$, and then the equation for a becomes linear:

$$\partial_t a=D_a\nabla^2 a-kb^*a. \quad (15)$$

This equation is supplemented with the following boundary conditions

$$a(x\rightarrow\infty, t)=0, \quad \left. \frac{\partial a}{\partial x} \right|_{x=0}=-\frac{a_0}{\sqrt{\pi D_a t}}. \quad (16)$$

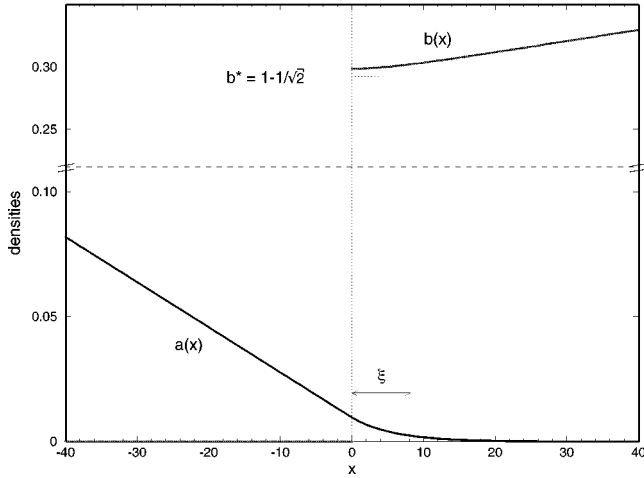


FIG. 3. Magnified view of the reaction zone shown in Fig. 2. Here the x coordinate is not scaled by $t^{1/2}$. The penetration length of particles A into the B region is shown by ξ . Note that there is a break in the vertical scale. The units are those defined in Fig. 1.

The second condition comes from the fact that the diffusion current entering the reaction zone at $x=0$ must be equal to that calculated from the macroscopic ($x \sim \sqrt{t}$) considerations.

Due to the slowness of diffusion, $a(x,t)$ changes slowly at large times, and one can consider quasistatic approximation. Looking for a solution of the form

$$a(x,t) \approx \frac{1}{\sqrt{t}} \Phi(x) \quad (17)$$

one can see that the left-hand side of Eq. (15) is of the order $t^{-3/2}$, while the right-hand side is proportional to $t^{-1/2}$, and so the time derivative can be neglected. The resulting equation for Φ can be easily solved, and the boundary conditions can be satisfied yielding a solution in a scaling form,

$$\frac{a(x,t)}{a_0} = \Psi(x/\xi, D_a t / \xi^2) = \frac{e^{-x/\xi}}{\sqrt{\pi D_a t / \xi^2}}, \quad (18)$$

where the penetration (or correlation) length is given by

$$\xi = \left(\frac{D_a}{k b^*} \right)^{1/2} \sim |r|^{-1/2}. \quad (19)$$

Since $b(x,t) \approx b^*$ in the reaction zone, we can obtain $R(x,t)$ from Eq. (18):

$$R(x,t) = kab \approx kab^* \sim \frac{a_0 D_a}{\sqrt{\pi D_a t}} \frac{e^{-x/\xi}}{\xi}, \quad x > 0, \quad (20)$$

$$= 0, \quad x < 0. \quad (21)$$

Thus the reaction rate goes down with time as $1/\sqrt{t}$, while the center and the width of the reaction zone remain finite in this scaling limit,

$$x_f \sim w \sim \xi. \quad (22)$$

One can see from Fig. 4 that the scaling form (18) agrees

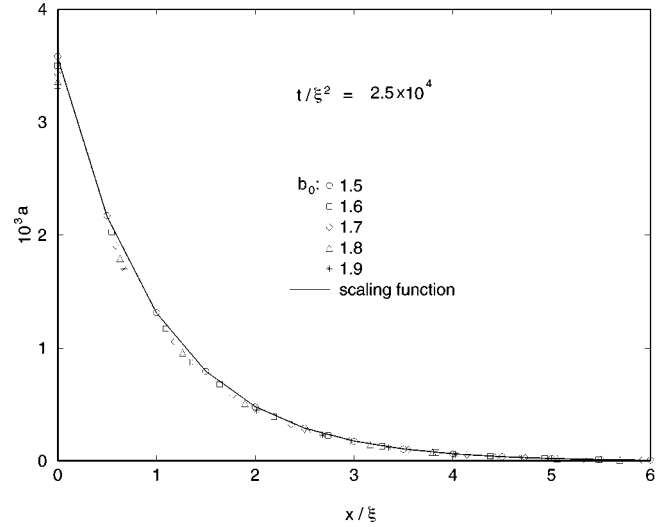


FIG. 4. Scaling of the density of A 's in the reaction zone shown in Fig. 2. The parameters are the same as in Fig. 2, except for t and b_0 , which are varied in order to keep t/ξ^2 constant [ξ is given by Eq. (19)]. The numerical solution of the full set of reaction-diffusion equations [Eqs. (2) and (3)] is compared with the quasi-stationary scaling solution Φ_a (solid line). Since one has $b \approx b^*$ in the reaction zone, the scaling function of the reaction rate $R = kab = \approx kab^*$ is proportional to that of a . The units are those defined in Fig. 1.

with the scaling obtained from the numerical solution of the full set of equations (2) and (3).

The phase considered above may be called the phase of localized reaction zone. One can observe from Eq. (19), however, that ξ diverges as we approach the $r=0$ point and thus the reaction zone becomes delocalized at $r=r_c=0$. Thus r plays the role of the distance from a critical point and the exponent we found, $\xi \sim r^{-\nu} \sim r^{-1/2}$ is obviously the mean-field exponent $\nu = \frac{1}{2}$ in accord with the neglect of fluctuations in the above description.

C. $r=0$: Localization-delocalization transition—critical front

It follows from Sec. III B that the $r=0$ case can be considered as a critical point which separates the localized and delocalized phases. Thus we expect that a scaling description is valid again at $r=r_c=0$ but, in expressions like Eq. (18), the correlation length must be replaced by a time-dependent correlation length which scales as a power of time, $\xi(t) \sim t^\alpha$. In order to see that this picture is valid, we follow the steps of Sec. III B: the problem is first solved on the diffusion scale [the solution is actually given by Eqs. (12) and (13) with $b^*=0$] and then matching solution in the $x \approx 0$ region is found (Figs. 5 and 6).

In the $x \approx 0$ region we seek scaling solutions suggested by Eq. (18)

$$a(x,t) \approx \frac{\Phi_a(x/t^\alpha)}{t^{1/2-\alpha}}, \quad b(x,t) \approx \frac{\Phi_b(x/t^\alpha)}{t^{1/2-\alpha}}. \quad (23)$$

Several comments are in order to clarify the above scaling assumptions. First, the scaling of x by the same t^α in Φ_a and Φ_b is the assumption that there is only one length scale governing the reaction zone. Second, the exponent α should be

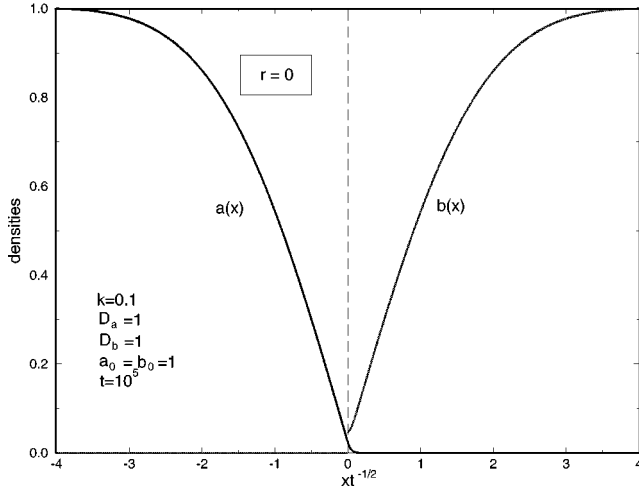


FIG. 5. Density profile of the reagents at the critical point ($r=0$) as seen on a diffusive scale ($x \sim t^{1/2}$). Notation is explained in the caption to Fig. 2. The units are those defined in Fig. 1.

$\frac{1}{6}$ or less since the case without the membrane gives an upper limit for the spread of the reaction zone, and there the width is proportional to $t^{1/6}$. Finally, one should note that the exponent $\frac{1}{2} - \alpha$ of the prefactors of the scaling functions is, in principle, an independent exponent. In this case, however, it is fixed by the boundary condition $(\partial a / \partial x)_{x=0} \sim 1/\sqrt{t}$ and by the requirement that the large-argument asymptotics of $b(x, t)$ should match the solution obtained on the $x \sim \sqrt{t}$ scale.

Substituting the scaling forms (23) into Eqs. (2) and (3), one finds that, for large times and for $\alpha < \frac{1}{2}$, the time derivatives on the left-hand sides can be neglected. Furthermore, the right-hand sides yield meaningful equations only if α is set to $\alpha = \frac{1}{6}$. The resulting equations then take the forms

$$\frac{d^2 \Phi_a}{dz^2} = \frac{k}{D_a} \Phi_a \Phi_b, \quad (24)$$

$$\frac{d^2 \Phi_b}{dz^2} = \frac{k}{D_b} \Phi_a \Phi_b, \quad (25)$$

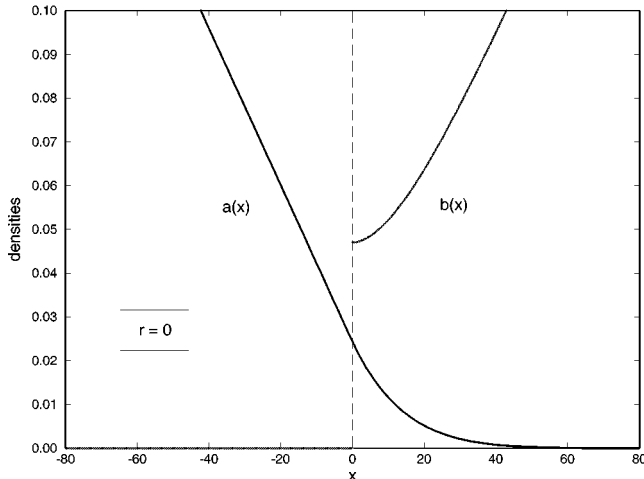


FIG. 6. Magnified view of the reaction zone shown in Fig. 5. Note that here x is not scaled by $t^{1/2}$. The units are those defined in Fig. 1.

where the scaling variable is $z = x/t^{1/6}$.

The boundary conditions to the above equations follow from $a(x \rightarrow \infty, t) = 0$ and $\partial b / \partial x(0^+, t) = 0$, and from matching the solutions to the ones found on the diffusive scale

$$\Phi_a(z \rightarrow \infty) = 0, \quad \left. \frac{d\Phi_a}{dz} \right|_{z=0} = -\frac{a_0}{\sqrt{\pi D_a}}, \quad (26)$$

$$\left. \frac{d\Phi_b}{dz} \right|_{z=0^+} = 0, \quad \left. \frac{d\Phi_b}{dz} \right|_{z \rightarrow \infty} = \frac{b_0}{\sqrt{\pi D_b}}. \quad (27)$$

Equations (24) and (25) with boundary conditions (26) and (27), however, pose a difficulty related to the fact that the combination $v = D_a \Phi_a - D_b \Phi_b$ satisfies a linear equation $v'' = 0$, and the solution $v = Pz + Q$ contains an integration constant Q which is not determined by the boundary conditions. Consequently, the scaling functions do not appear to be unique.

This problem of uniqueness can be dealt with by returning to the diffusive scale $x \sim \sqrt{t}$, and reexamining the solutions found there. We shall demonstrate the idea on the example of a system where $D_a = D_b$ (and $a_0 = b_0$, since we are at criticality). In this case, $u = a - b$ satisfies the diffusion equation for both $x > 0$ and $x < 0$, the boundary conditions are given by $u(-\infty, t) = -u(\infty, t) = a_0$ and $\partial_x u(0^-, t) = \partial_x u(0^+, t)$ and, furthermore, the initial condition $[u(x < 0, 0) = a_0; u(x > 0, 0) = -a_0]$ is an odd function of x . It follows then that the solution is an odd function, $u(x, t) = -u(-x, t)$. Next we note that $u = a$ for $x < 0$ while $u = a - b$ for $x > 0$, and, approaching $x = 0$ from both sides, the oddness of u yields the following relationship:

$$-a(x=0^-, t) = a(x=0^+, t) - b(x=0^+, t). \quad (28)$$

Since there is no accumulation of A particles at $x = 0$, we have $\partial a(x=0^-, t) = \partial a(x=0^+, t)$ and, consequently, a is continuous function across the membrane, $a(x=0^-, t) = a(x=0^+, t)$. Then Eq. (28) yields $b(0, t) = 2a(0, t)$, which, in turn, provides an additional boundary condition for the scaling functions:

$$\Phi_b(0) = 2\Phi_a(0). \quad (29)$$

The same extra boundary condition can also be found for $D_a \neq D_b$, but the argument is rather involved, so we shall not reproduce it here. From the perspective of critical phenomena, it is quite natural that the scaling function does not depend on such details as the diffusion coefficients.

Having the extra boundary condition (29), Φ_a and Φ_b can now be found numerically. Some properties of the scaling functions can, however, be seen by just inspecting the equations. For example, substituting the large- z asymptotics $\Phi_b(z) \sim z$ into Eq. (24), one can see that $\Phi_a(z \rightarrow \infty)$ is given by the Airy function [30].

In Fig. 7, we show that the scaling regime does exist, and that the numerical results do agree with the solution of the full equations (2) and (3). It then follows from Eqs. (24) and (25) that the production rate can also be written in a scaling form

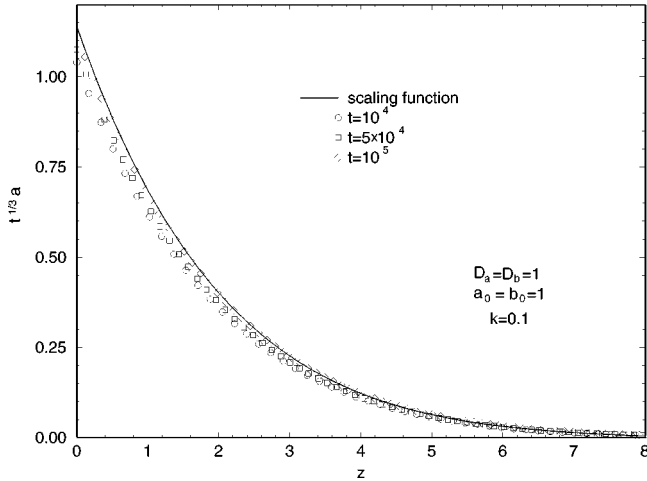


FIG. 7. Scaling function Φ_a for a [Eq. (23)]. The numerical solution of the full set of reaction-diffusion equations [Eqs. (2) and (3)] is compared with the quasistationary scaling solution. The units are those defined in Fig. 1.

$$R(x,t) \sim \frac{1}{t^{2/3}} \Phi_a\left(\frac{x}{t^{1/6}}\right) \Phi_b\left(\frac{x}{t^{1/6}}\right) = \frac{1}{t^{2/3}} \Psi\left(\frac{x}{t^{1/6}}\right), \quad (30)$$

and we can observe that the reaction front remains attached to the wall, but that it expands with time into the $x > 0$ region. Both the center and width of the zone diverge with time as

$$x_f \sim w \sim t^{1/6}, \quad (31)$$

and both exponents are the same in contrast to the delocalized phase where $x_f \sim t^{1/2}$ and $w \sim t^{1/6}$.

IV. IMPORTANCE OF FLUCTUATIONS

The above discussion is based on a mean-field-like treatment, and one can ask what is the role played by the fluctuations. In the case without a semipermeable wall, it has been shown [6,13] that the upper critical dimension above which the mean-field theory is correct is $d_u = 2$. In dimension $d = 1$, the critical exponents take their non-mean-field values. For example, the width exponent changes from the mean-field value $\alpha = \frac{1}{6}$ to $\frac{1}{4}$. As we saw before, the above situation corresponds to the case of a delocalized front $r > 0$. For the critical case, $r = 0$, we performed cellular automata numerical simulations. Details on this type of simulations can be found in Ref. [5]. One considers the synchronous random walk of two types of particles (representing species A and B) on a regular lattice. At time $t = 0$, the A and B particles occupy the left and right halves of the lattice, respectively. Upon encounter, an A and a B particle annihilate. This reaction process, as well as the diffusion mechanism, were described in more detail in Refs. [5,6]. Here we consider one- and two-dimensional systems, with a semipermeable membrane located at the $(x=0, y)$ plane. When a B particle hits the semipermeable wall it bounces back, while the A particles are not affected. For the one-dimensional case we considered a chain of 2048 sites, while, for the two-dimensional case, the size of the system was 512×64 .

From a statistical point of view, it is better to study nu-

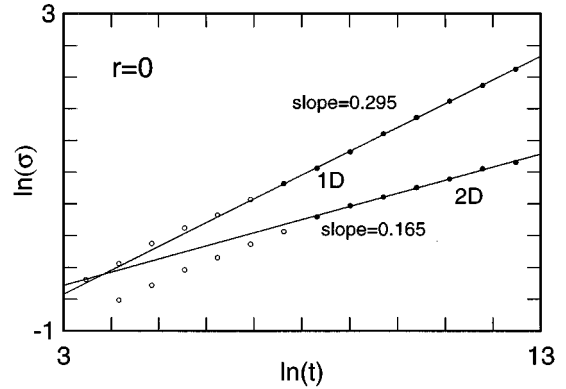


FIG. 8. Width of the cumulative production rate $c(x,t)$ for a cellular automata dynamics, in one- and two-dimensional systems. The width exponents, given by the slope of the log-log plot, are compatible with the expected values $\alpha = \frac{1}{4}$ and $\frac{1}{6}$. Time is measured in units of computation steps, while the width is given in units of lattice spacing.

merically the cumulative production rate, defined as

$$c(x,t) = \int_0^t d\tau R(x,\tau) \quad (32)$$

in one dimension. In two dimensions, the production rate also depends on the transverse coordinate y , and we define $c(x,t)$ as an average over the y direction:

$$c(x,t) = \int_0^t \int dy d\tau R(x,y,\tau). \quad (33)$$

Assuming the scaling form given by Eq. (9) for the production rate R , it follows that the above cumulative production rates $c(x,t)$ have the same width and mean position exponent α as R .

In Fig. 8, the widths σ of the cumulative production rates are shown as a function of time t . The quantity σ is computed as the width (7) but with $c(x,t)$ replacing $R(x,t)$. The values of the exponent α are 0.295 ± 0.010 and 0.165 ± 0.010 , respectively, in one and two dimensions. The values agree with the ones found in the case without a semipermeable wall [5,6]. Whereas the two-dimensional exponent fits well with its theoretical value $\frac{1}{6}$, the one-dimensional situation is not as satisfactory. Nevertheless, as argued in Ref. [13], it is very difficult to obtain the theoretical value $\alpha = \frac{1}{4}$ from a simulation of the time dependence of the width.

Finally, a log-log plot of the mean position of the front versus time yields exponents whose values are in agreement with the above results, namely, $\alpha = 0.252 \pm 0.010$ in one dimension and $\alpha = 0.163 \pm 0.010$ in two dimensions. Thus we conclude that the fluctuations play a similar role for both cases $r = 0$ and $r > 0$.

V. FINAL REMARKS

We can now summarize the properties of the localization-delocalization transition discussed above as follows. For $r < 0$, the reaction zone is localized at the membrane, and the width is determined by the correlation length, ξ , describing

the penetration of the A particles into the constant-density B region. At $r=0$ the penetration length diverges, but there is still a single (diverging with time) length which characterizes the reaction zone. It should be noted that a diverging diffusion length $\ell_D \sim \sqrt{t}$ is always present, but it is irrelevant for $r \leq 0$. For $r > 0$, however, the diffusion length starts to play a role: the reaction zone becomes delocalized and two distinct length scales appear. One of them is the distance of the center of the zone from the membrane, $x_f \sim \sqrt{t}$, which is just the diffusion length while the other is the width of the reaction zone, $w \sim t^{1/6}$ (in the mean-field approximation).

The questions of how much C is produced near the membrane, and whether their density c grows to exceed some aggregation threshold c_0 , may be of importance in biological phenomena (e.g., in the building of rather intricate but regular mineral skeletons of single-cell organisms such as radiolaria [28] or diatoms [29]). The answers to the above questions depend on the localization properties of the reaction zone.

For $r < 0$, the reaction zone has a finite width and thus, provided the C 's do not diffuse away, their density will increase with time as $c(t) \sim \sqrt{t}$. This result follows from the fact that the current $J^A(t)$ of A particles toward the reaction zone is proportional to $1/\sqrt{t}$ and, consequently, the amount of C 's, produced up to time t , is given by $M_C \sim \int^t J^A(\tau) d\tau \sim \sqrt{t}$.

A somewhat slower increase of $c(t)$ takes place at $r=0$. Since the width of the reaction zone diverges as $w \sim t^{1/6}$, one finds $c(t) \sim M_C/w \sim t^{1/3}$. We can see that, for both $r < 0$ and $r=0$, the density of C 's near the membrane exceeds any threshold c_0 at sufficiently large times. Thus supersaturation and, associated with it, the precipitation of C may occur in these regimes.

Finally, for $r > 0$, the reaction zone leaves the membrane and only a finite density of C 's left behind. The actual value of this density depends sensitively on the initial conditions and one cannot make statements about possible precipitation

without a knowledge of the actual parameters.

The above considerations, of course, do not constitute an attempt toward an explanation of a real biological phenomena such as the precipitation of the siliceous structures of single-cell radiolaria. This is so even if one imagines that, at the early stages of the evolution, the regular skeletons are either produced as an instability in a physicochemical, reaction-diffusion process, or arise by surface-tension-assisted precipitation where the membranes are present but play a passive role (their intersections define the precipitation regions) [31]. At the present stage of evolution, the skeletons are covered with a membranous cytoplasmic sheet which appears to play an important role (e.g., transport along the membrane) in the skeletal depositions [28]. Thus any attempt at a *physicochemical* explanation should include the presence of such an *active* membrane near the precipitation zone.

In this paper, we derived results for the properties of reaction zones near a semipermeable membrane which is *active* only in the sense that it is blocking the transport of one of the reagents. We hope, however, that our results will help in discussing more complicated reactions near *active* membranes in the same way as the understanding of the properties of the reaction zone [1] in the $A+B \rightarrow C$ reaction helped in elucidating the features of the pattern formation in the much more complicated Liesegang phenomena [22].

ACKNOWLEDGMENTS

This work was partially supported by the Swiss National Science Foundation in the framework of the Cooperation in Science and Research with CEEC/NIS, by the Hungarian Academy of Sciences (Grant No. OTKA T 019451), and by an EC Network Grant ERB CHRX-CT92-0063. Z.R. would like to thank the members of the Theoretical Physics Department for the hospitality during his stay at the University of Geneva.

-
- [1] L. Gálfi and Z. Rácz, Phys. Rev. A **38**, 3151 (1988).
 [2] Y. E. Lee Koo, L. Li, and R. Kopelman, Mol. Cryst. Liq. Cryst. **183**, 187 (1990).
 [3] Z. Jiang and C. Ebner, Phys. Rev. A **42**, 7483 (1990).
 [4] Y. E. Lee Koo and R. Kopelman, J. Stat. Phys. **65**, 893 (1991).
 [5] B. Chopard and M. Droz, Europhys. Lett. **15**, 459 (1991).
 [6] S. Cornell, B. Chopard, and M. Droz, Phys. Rev. A **44**, 4826 (1991).
 [7] H. Taitelbaum, S. Havlin, J. E. Kiefer, B. Trus, and G. H. Weiss, J. Stat. Phys. **65**, 873 (1991).
 [8] F. Leyvraz and S. Redner, Phys. Rev. Lett. **66**, 2168 (1991); J. Stat. Phys. **65**, 1043 (1991).
 [9] E. Ben-Naim and S. Redner, J. Phys. A **25**, L575 (1992).
 [10] M. Araujo, S. Havlin, H. Larralde, and H. E. Stanley, Phys. Rev. Lett. **68**, 1791 (1992).
 [11] H. Larralde, M. Araujo, S. Havlin, and H. E. Stanley, Phys. Rev. A **46**, 855 (1992).
 [12] H. Taitelbaum, Y. E. Lee Koo, S. Havlin, R. Kopelman, and G. H. Weiss, Phys. Rev. A **46**, 2151 (1992).
 [13] S. Cornell and M. Droz, Phys. Rev. Lett. **70**, 3824 (1993).
 [14] M. Howard and J. Cardy, J. Phys. A **28**, 3599 (1995).
 [15] G. T. Barkema, M. J. Howard, and J. L. Cardy, Phys. Rev. E **53**, R2017 (1996).
 [16] S. Cornell, Z. Koza, and M. Droz, Phys. Rev. E **52**, 3500 (1995).
 [17] Z. Koza and H. Taitelbaum, Phys. Rev. E **54**, R1040 (1996).
 [18] Z. Koza, J. Stat. Phys. **85**, 179 (1996).
 [19] E. L. Cabarcos, C.-S. Kuo, A. Scala, and R. Bansil, Phys. Rev. Lett. **77**, 2834 (1996).
 [20] J. S. Langer, Rev. Mod. Phys. **52**, 1 (1980).
 [21] G. T. Dee, J. Stat. Phys. **39**, 705 (1985); Phys. Rev. Lett. **57**, 275 (1986).
 [22] B. Chopard, P. Luthi, and M. Droz, Phys. Rev. Lett. **72**, 1384 (1994); J. Stat. Phys. **76**, 661 (1994).
 [23] M. C. Cross and P. C. Hohenberg, Rev. Mod. Phys. **65**, 851 (1993).
 [24] B. Chopard, M. Droz, and L. Frachebourg, Int. J. Mod. Phys. **5**, 47 (1994).

- [25] A. Büki, É. Kárpáti-Smidróczki, and M. Zrínyi, *J. Chem. Phys.* **103**, 10 387 (1995).
- [26] M. J. E. Richardson and M. R. Evans, *J. Phys. A* **30**, 811 (1997).
- [27] D. W. Fawcett, *The Cell* (Saunders, London, 1981).
- [28] O. R. Anderson, *Radiolaria* (Springer-Verlag, New York, 1983).
- [29] *Silicon and Siliceous Structures in Biological Systems*, edited by T. L. Simpson and B. E. Volcani (Springer-Verlag, New York, 1981).
- [30] *Handbook of Mathematical Functions*, edited by M. Abramowitz and I. A. Stegun (Dover, New York, 1965).
- [31] D'Arcy W. Thompson, *On Growth and Form* (Macmillan, New York, 1942).